Korean J. Chem. Eng., 40(10), 2455-2462 (2023)
DOI: 10.1007/s11814-023-1474-3

pISSN: 0256-1115
eISSN: 1975-7220

Investigating the effect of solvent composition on ink structure and crack formation in polymer electrolyte membrane fuel cell catalyst layers

Seong Hyeon Woo*,, Sungmin Kim*,**, Seunghee Woo*, Seok-Hee Park*, Yun Sik Kang*, Namgee Jung**,†, and Sung-Dae Yim*,†**

*Fuel Cell Laboratory, Korea Institute of Energy Research (KIER), 152, Gajeong-ro, Yuseong-gu, Daejeon 34129, Korea
**Graduate School of Energy Science and Technology (GEST), Chungnam National University, 99 Daehak-ro, Yuseong-gu, Daejeon 34134, Korea
(*Received 9 March 2023 • Revised 28 March 2023 • Accepted 17 April 2023*)

Abstract−To improve the performance of polymer electrolyte membrane fuel cells (PEMFCs), controlling the microstructure of the membrane electrode assembly (MEA) catalyst layer is crucial. Ink design, which includes a catalyst, an ionomer, and a solvent, serves as the starting point for controlling the microstructure of the catalyst layer. However, there is a significant lack of understanding of the ink structure required for this purpose. In this study, we investigated the effect of the solvent, a key component that determines the ink structure. The ink comprises 20 wt% Pt/C, short-side-chain (SSC) Aquivion ionomer, and a solvent mixture of 1-propanol (NPA) and water. Three types of inks with different compositions of NPA and water are manufactured, and their stability and rheological properties were measured to infer and compare the ink structures. Furthermore, the crack characteristics of the catalyst layer were compared by directly coating the ink onto the electrolyte membrane using the doctor-blade method. In the ink with a high water content, we observed a gel-like elastic behavior dominated by network structures formed by ionomers adsorbed between catalyst particles. In contrast, the ink with a high NPA content exhibited a liquid-like viscous behavior dominated by well-dispersed catalyst particles and ionomers. These properties of the inks directly influence the crack formation characteristics after coating. Specifically, the strong liquid properties of the NPA-rich ink were found to suppress crack formation in the catalyst layer. These findings provide important insights into how the solvent composition affects ink structure and how it, in turn, influences crack formation in the catalyst layer, which can help optimize the ink design to improve the performance of PEMFCs.

Keywords: Fuel Cell, PEMFC, Ink, Catalyst Layer, Crack

INTRODUCTION

A polymer electrolyte membrane fuel cell (PEMFC) is a clean and efficient energy conversion system that turns hydrogen's chemical energy into electrical energy. A key component of this system is the membrane electrode assembly (MEA), which performs the electrochemical reactions necessary for energy conversion and directly affects the cell's performance and durability. The MEA consists of a catalyst layer coated on both sides of a polymer electrolyte membrane (PEM). The catalyst layer is made up of platinum catalyst supported on carbon and ionomer. For the oxygen reduction reaction (ORR) to occur in the catalyst layer, the transfer of oxygen gas, hydrogen ions, and electrons to the catalyst surface where the reaction takes place must be fast. The transfer rate of these three reactants depends on the microstructure of the catalyst layer, which is directly related to the performance of the MEA. The catalyst layer is formed through a series of processes such as coating, drying, and heat treatment starting from an ink composed of catalyst, ionomer, and solvent. Therefore, the ink directly affects the final structure of the catalyst layer, and many efforts are being made to understand the key physical phenomena that determine the structure.

To understand the interactions between catalyst-ionomer-solvent that make up the ink, various analysis methods have been used, such as SANS [1-3], USAXS [4-7], DLS [8-11], Cryo-TEM [4,7,12], and QCM [13]. In addition, simulation studies based on MD have also been carried out to effectively interpret these experimental and analytical results [14-17]. However, these analysis techniques have limitations in providing information on the actual ink situation, as they often apply a two-component ink with minimized variables such as catalyst/solvent or ionomer/solvent, and sometimes provide information on samples obtained after ink drying. Therefore, recent studies have focused on inferring the structure of actual inks through sedimentation behavior or rheological properties. For example, Kumano et al. showed that solvent properties can significantly change the ink and catalyst layer structure by observing the differences in rheological properties and crack characteristics of inks prepared with different solvents [9]. Khandavalli et al. systematically investigated the viscosity properties of inks with different ionomer content using two types of widely used catalysts in fuel cells, Pt/VC and Pt/K [18]. Hoffmann et al. introduced carbon particles with different pore characteristics as model catalysts, prepared inks with different ionomer content, and conducted various measurements, such as ink stability, rheological properties, and crack characteristics, to find correlations between ink and catalyst layer structures [19].

†To whom correspondence should be addressed.
E-mail: njung@cnu.ac.kr, jimmyim@kier.re.kr

Despite these efforts, there is still a lack of a comprehensive database of research results to establish a theoretical foundation for ink design due to the diversity of materials that make up the ink, such as the characteristics of the catalyst (crystallinity of carbon support, surface area, pore characteristics, loading of platinum, location of platinum particles inside/outside of carbon pores, etc.), the structure of the ionomer (length of side chains, IEC value, etc.), the properties of the solvent (water, NPA, IPA, NMP, PG, Glycerin, etc.), and the various variables in the ink manufacturing process (mixing, grinding, dispersion, equipment and operation time/number in each process, etc.).

In this study, Pt/C catalyst containing 20 wt% platinum supported on high-crystallinity carbon was used, with short-side-chain (SSC) Aquivion as the ionomer, and a solvent mixture of 1-propanol (NPA) and water for ink preparation. The solvent composition was varied by changing the content of water and NPA to observe the effect on ink stability, rheological properties, and cracking behavior in the catalyst layer. Based on the observations, the ink structure and crack formation mechanism dependent on the composition of water and NPA were proposed. This study is expected to contribute to the understanding of the interaction between catalyst, solvent, and ionomer for ink structure design and the ink transfer process to the catalyst layer.

EXPERIMENTAL

1. Ink Preparation

For the ink catalyst, we utilized commercially available platinum catalyst supported on highly crystalline carbon support (Pt/C, 19.8 wt% Pt, TEC10EA20E, Tanaka Kikinzoku). The ionomer was supplied in the form of a dispersed solution of short-side-chain (SSC) perfluorosulfonic acid (PFSA) polymer with a concentration of 25 wt% in water (Aquivion D83-24BS, Solvay). The solvent used was a mixture of water and 1-propanol (NPA), prepared at varying ratios of NPA to water (20, 50, and 72 wt% NPA). The inks prepared with different solvent compositions were named NPA20, NPA50, and NPA72, and their detailed compositions are summarized in Table 1. It is important to note that the maximum NPA content of NPA72 was determined based on the minimum water required for catalyst wetting, fixed solid content, and I/C values. The solid content of the ink, consisting of the catalyst and ionomer, was set at 20 wt%, while the I/C value was set to 0.8. The ink containing all three components was prepared through a series of processes, including ultrasonication (POWER SONIC 405), planetary mixing (THINKY, ARE-310), high shear mixing (SILVERSON, L5M-A), and nano dispersion (ILSHIN AUTOCLAVE, NLM 100-Z75).

2. Ink Sedimentation Behavior Analysis

The sedimentation behavior of the ink over time was measured using an analytical centrifugation instrument (LUMiSizer® 610, LUM GmbH). The device is designed to accelerate particle settling in the sample by applying centrifugal force, allowing for the measurement of ink stability over a short period of time. During centrifugation, monochromatic light is periodically injected into the cell, and the attenuated light intensity, which is detected as the ink passes through, is measured, thereby determining the changes in transmittance and sedimentation behavior. The raw transmittance data obtained were plotted and interpreted as sedimentation behavior according to the method reported by Bapat and Segets [20]. Approximately 1.5 mL of ink was extracted using a micro-pipette and injected into a 10 mL glass cuvette, which was then positioned in the device chamber. The chamber temperature was maintained at 25 °C throughout the analysis. The centrifugal force was applied at 2900 RPM (1,200 ×g at a mean rotational radius of 130 mm), and 1000 transmittance values were obtained by injecting light at a wavelength of 870 nm into the cuvette every 60 seconds. The total operation time ranged from 3 to 17 hours depending on the sedimentation rate of the sample.

3. Ink Rheological Characterization

The rheological properties of the ink were measured using a rheometer (MCR102e, Anton Paar) with a cylinder double gap (Bob active length: 40 mm, Bob inner diameter: 25 mm, Bob outer diameter: 27 mm, Cup inner diameter: 23 mm, Cup outer diameter: 29 mm). The viscoelastic behavior was measured using an amplitude sweep test and a frequency sweep test. In the amplitude sweep test, the angular frequency was fixed at 10 rad/s, and the range of shear strain was applied from 0.01 to 100% to measure the storage modulus G′ and the loss modulus G″. Then, a recovery of 5 minutes was allowed for the ink to recover from the deformation caused by strain. Next, in the frequency sweep test, the shear strain value was fixed at 0.68%, which was within the linear viscoelastic region (LVE) range measured in the amplitude sweep test, and G′ and G″ were measured at angular frequencies ranging from 200 to 0.1

Table 1. Specifications of prepared inks and ionomer dispersions

Sample name	Catalyst (wt%)	Ionomer (wt%)	Solvent (wt%)	NPA/water ratio (w/w)	NPA/water ratio (mol/mol)
NPA20	12.2	7.8	80	1 : 4	1 : 13.6
NPA50	12.2	7.8	80	1 : 1	1 : 3.3
NPA72	12.2	7.8	80	2.6 : 1	1.2 : 1
NPA20_C	3	0	97	1 : 4	1 : 13.6
NPA50_C	3	0	97	1 : 1	1 : 3.3
NPA72_C	3	0	97	2.6 : 1	1.2 : 1
NPA20_I	0	7.8	92.2	1 : 4	1 : 13.6
NPA50_I	0	7.8	92.2	1 : 1	1 : 3.3
NPA72_I	0	7.8	92.2	2.6 : 1	1.2 : 1

rad/s. A recovery of 5 minutes was performed again. Finally, viscosity measurements were performed by applying a range of shear rates from 0.01 to 3,800 s^{-1}. All rheological characterization was carried out at 25 °C.

4. Ink Coating and Catalyst Layer Crack Analysis

Direct doctor blade coating of ink onto the surface of the electrolyte membrane was employed. Nafion (NR-211, Chemours) was used as the electrolyte membrane. The membrane was placed on a vacuum suction and heating plate and vacuum was applied to ensure the membrane was tightly adhered to the plate. A certain amount of ink was dropped onto the Nafion, and then coated horizontally using a 4 path film applicator at a coating speed of 10 mm/s and a coating gap of 50 μm. The coating area of the catalyst layer was controlled using masking film to achieve 25 cm^2. The ink coating process was performed at room temperature without any temperature control on the heating plate, and the drying after coating was also carried out at room temperature for 1 h. The crack morphology on the surface of the prepared catalyst layer was measured using a microscope (ICAMSCOPE, SOMETECH) with a magnification of 300x. The platinum loading at each point was measured using a portable XRF (Niton XL5 Plus, Thermo Scientific) to confirm the platinum distribution and coating uniformity in nine parts of the catalyst layer. The average platinum loading was 0.1 mg/cm^2.

RESULTS AND DISCUSSION

The ink used for manufacturing the catalyst layer of MEA for fuel cells, which is typically composed of catalyst, ionomer binder, and solvent, is prepared through several dispersion processes of these components. During this preparation process, the components of the ink interact with each other to form a structure. The interaction between the catalyst and solvent determines the size of the catalyst aggregation, the interaction between the ionomer and solvent determines the size and shape of the ionomer, and the interaction between the catalyst and ionomer affects the adsorption form of the ionomer on the catalyst surface, thus altering the ink structure [13,21]. Ultimately, the final structure of the ink is determined by interactions that minimize the free energy of the ink system. One way to examine the ink structure is to utilize sedimentation behavior and rheological properties of the ink. In this study, we investigated the sedimentation behavior of the ink to determine the structural changes resulting from changes in solvent composition for ink used in fuel cell systems.

1. Ink Sedimentation Behavior

First, we observed the change in affinity between the solvent and catalyst due to changes in the solvent composition. We prepared three types of inks consisting only of catalyst and solvent without

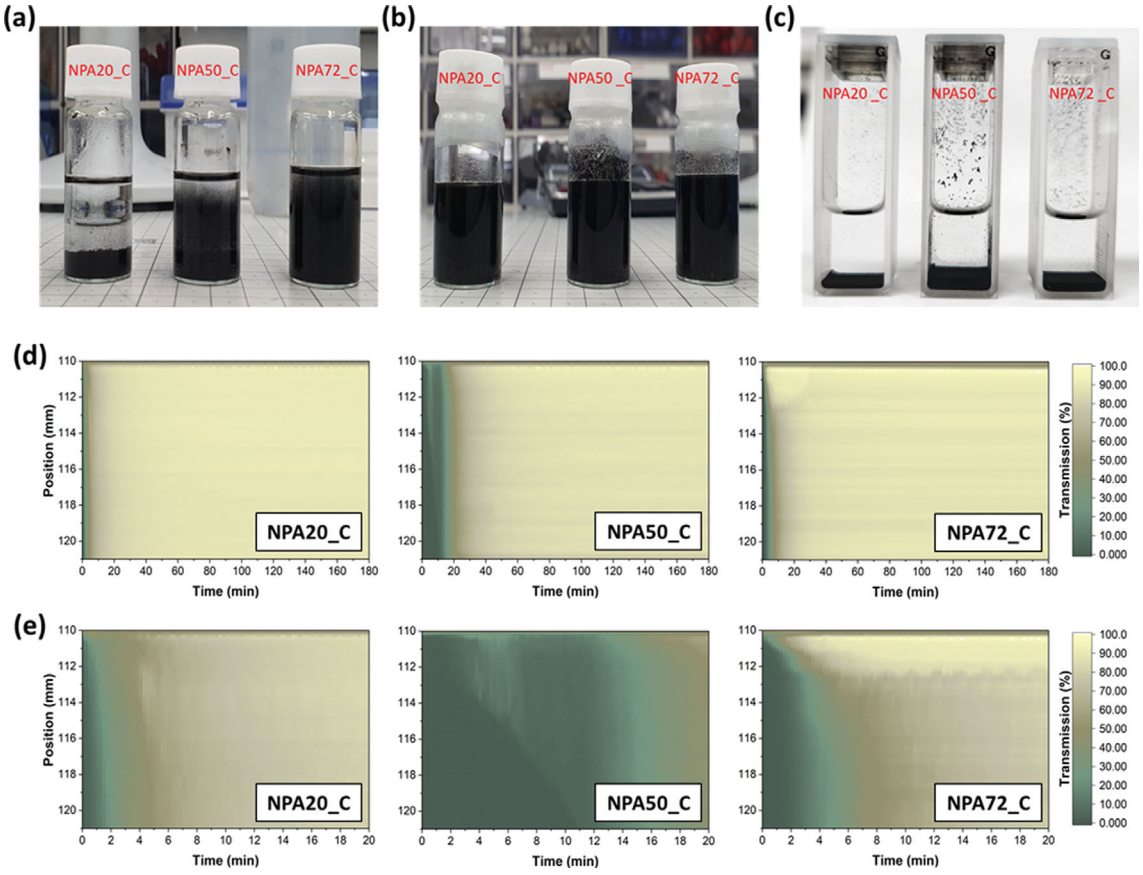

Fig. 1. Ink manufactured only with catalyst and solvent without the addition of ionomer. Photographs showing the dispersion state of ink (a) before and (b) after ultrasonic treatment. (c) Photographs of ink in a glass cuvette obtained immediately after sedimentation experiment. Transmittograms obtained through sedimentation experiment of inks. (d) Overall results for 180 min and (e) results for the initial 20 min.

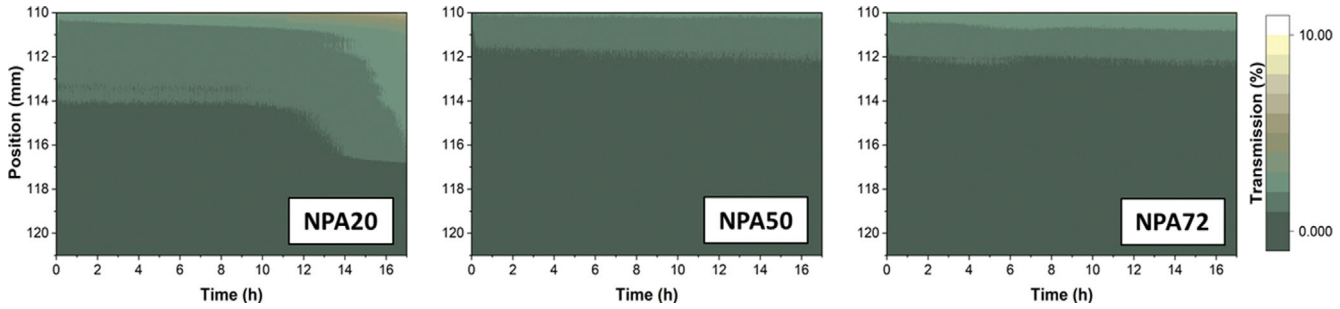

Fig. 2. Transmittograms obtained from a 17-hour sedimentation experiment of inks manufactured with the inclusion of ionomer.

the addition of ionomer, where the catalyst content was 3 wt%; the detailed ink compositions are summarized in Table 1. The inks were dispersed using an ultrasonic process, and stable inks could be obtained by applying ultrasound for 10 min and observing the ink within a short time range (Figs. 1(a), (b)). To observe the ink sedimentation behavior within a short time, we analyzed it by applying centrifugal force and measuring the change in light transmittance caused by the sedimentation of particles using equipment.

Fig. 1(d) shows a graph of the ink's light transmittance as a function of time when centrifugal force is applied, depending on the height of the cuvette cell. The change in shade of the cyan color represents the light transmittance at different positions and illustrates the settling behavior of the catalyst particles. In the experiment performed for a total of 180 min, all samples settled completely within 20 min, as can also be seen in the image in Fig. 1(c). When examining the settling behavior during the first 20 min based on the time it takes for the light transmittance at the bottom of the cell (121 mm) to reach 70%, as shown in Fig. 1(e), the ink stability was in the order of NPA50_C>NPA72_C>NPA20_C, with settling times of 1 min for NPA20_C, 15 min for NPA50_C, and 5 min for NPA72_C, indicating that the solvent property had a significant impact on the settling behavior of the catalyst. According to the classical DLVO theory that explains particle motion in colloids, if the electrostatic force between particles, which is determined by the solvent properties, is smaller than the van der Waals force, particles aggregate, causing them to become larger and leading to settling [22-24]. The settling velocity due to particle aggregation is expressed by Stoke's law as follows.

$$v = \frac{(\rho_g - \rho_s)ga^2}{18\mu} \quad (1)$$

Here, v is the sedimentation velocity, ρ_g is the density of particles, ρ_s is the density of the fluid, a is the radius of the particle, g is the acceleration due to gravity, and μ represents viscosity. According to this formula, the variables that determine the sedimentation velocity of particles are the particle size, the density difference between the particles and fluid, and the viscosity of the ink. Therefore, the difference in stability of the inks due to the solvent observed in Fig. 1(d), (e) can be attributed to the difference in particle aggregation rate over time. As explained by the DLVO theory, particle size is determined by the balance of van der Waals forces and electrostatic repulsion, each of which is composed of Hamaker's constant and zeta potential. Therefore, it can be interpreted that changes in solvent composition affect these values, causing variations in the size of aggregated catalyst particles and resulting in different sedimentation behaviors.

Several previous studies have reported that even a small amount of ionomer injection into catalyst ink greatly improves its stability. The ionomer injected into the ink is partially adsorbed onto the catalyst surface, increasing the electrostatic repulsion between catalyst particles due to the sulfonic acid groups at the end of the ionomer side chains. Additionally, the steric hindrance effect induced by the ionomer adsorbed on the catalyst particles enhances ink stability [10,11,25,26]. In this study, ionomers corresponding to I/C 0.8 were injected into catalyst ink systems consisting of three types of solvent compositions, and their centrifugal stability was measured for 17 h. The results are shown in Fig. 2. In all inks, even after 17 h of prolonged driving, a significant amount of catalysts exhibited stable behavior, clearly demonstrating that the presence of ionomers greatly enhances ink stability. Although NPA20 showed slightly lower stability than other inks, the difference was not significant. Compared with the results in Fig. 1 without ionomers, the presence of ionomers is clearly shown to significantly inhibit the aggregation of catalyst particles. In fact, the role of polymers as stabilizers in colloid systems has been reported for a long time [27], and research is ongoing to elucidate the interactions between particles, polymers, and solvents in colloid systems [28]. In ink systems for fuel cells, the degree of aggregation of ionomers and adsorption of catalysts varies depending on the solvent [21], but their influence on ink stability appears to be relatively minor. In ink systems including ionomers, there are limitations in examining differences in ink structure depending on the solvent only through ink sedimentation analysis, and therefore, the rheological characteristics of the ink were examined.

2. Ink Rheological Properties

Figs. 3(a)-(c) present graphs of viscosity measurements as a function of shear rate. The theoretical viscosity values of the NPA-water binary solvent ranged from 1 to 2 mPa·s, depending on the composition, which was confirmed experimentally. To systematically investigate the interactions among the three components that constitute the ink, we first examined the rheological properties of a two-component suspension comprising solvent-ionomer and solvent-catalyst. As shown in Fig. 3(a), the ionomer suspensions exhibit behavior close to that of a Newtonian fluid with a constant viscosity in the range of 0.1-0.01 Pa·s regardless of the shear rate. On the other hand, the catalyst dispersion exhibits high viscosity in the

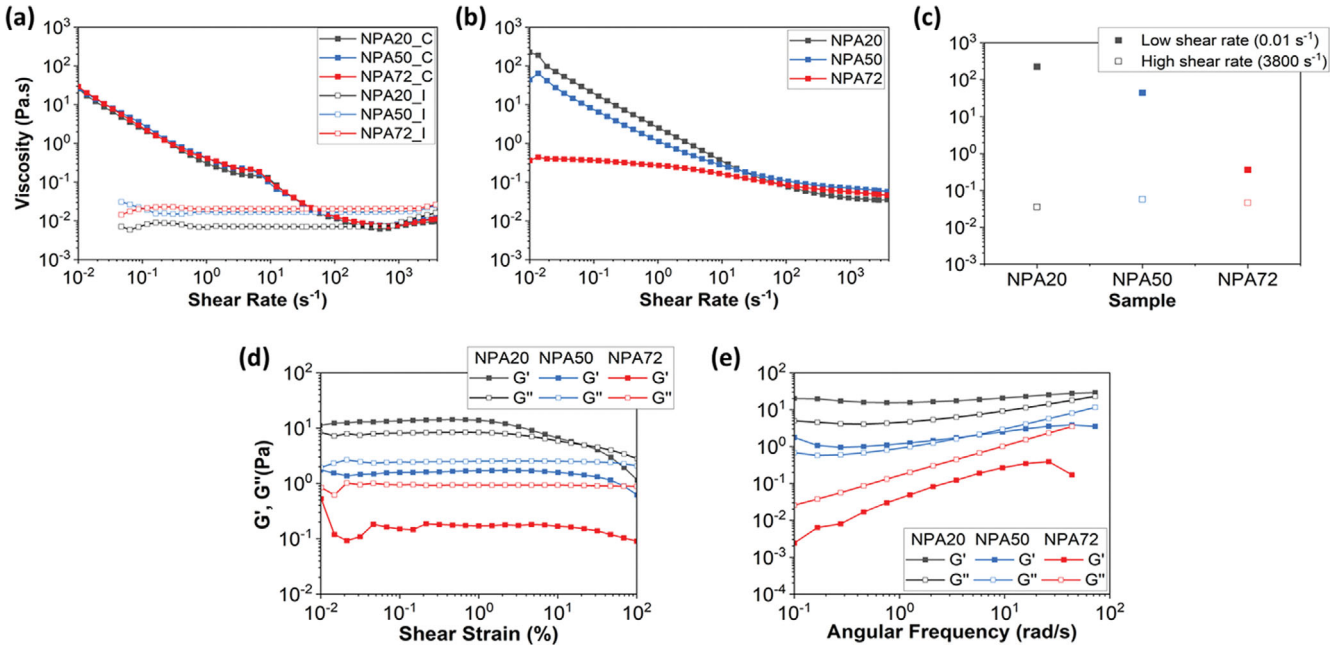

Fig. 3. Rheological characteristics of the prepared samples. (a) Viscosity curves for two-component suspensions composed of solvent-catalyst and solvent-ionomer. (b) Viscosity curves for inks composed of solvent-catalyst-ionomer. (c) Comparison of the viscosities of ink samples at low (0.01 s^{-1}) and high (3,800 s^{-1}) shear rates. Viscoelastic behavior measured by (d) amplitude scan and (e) frequency scan of inks.

range of 25-30 Pa·s at low shear rates, followed by shear-thinning behavior with decreasing viscosity as the shear rate increases. This is attributed to the aggregation and dispersion of the catalyst particles at low and high shear rates, respectively [18]. In ink formulations containing both catalyst and ionomer, as shown in Fig. 3(b), similar shear-thinning behavior to that of the solvent-catalyst system is observed. The shear-thinning behavior in three-component inks is also due to the aggregation and dispersion of catalyst particles, but the influence of the solvent is more significant in the presence of ionomer, resulting in a significant difference in viscosity and degree of shear thinning at low shear rates depending on the solvent composition (Figs. 3(b)-(c)). In particular, NPA72, which contains a large amount of NPA, exhibits behavior closer to that of a Newtonian fluid, with lower initial viscosity and less pronounced shear-thinning behavior than other inks. The ionomer itself has a negligible effect on the ink viscosity, but it is thought to primarily affect the agglomeration characteristics of the catalyst particles depending on the solvent composition, resulting in different rheological behaviors. When the water content is increased in the ink using a water/NPA mixed solvent, ionomers adsorbed onto the catalyst increase, while an increase in NPA content leads to the presence of more free ionomers that do not adsorb onto the catalyst [13,29]. Therefore, it is speculated that in NPA20 and NPA50, ionomers adsorbed onto the catalysts form a network structure due to interparticle forces, and shear thinning behavior occurs as this network structure is disrupted under strong shear forces. However, in NPA72, free ionomers interfere with the formation of a network structure between catalyst particles, leading to the occurrence of free-polymer-induced (FPI) stabilization and exhibiting low viscosity and Newtonian fluid behavior [28].

Fuel cell ink exhibits both viscous and elastic behavior, providing information on the ink's microstructure. Fig. 3(d) shows the ink's viscoelastic behavior under amplitude sweep testing. In comparison to the region showing linear viscoelastic (LVE) behavior, NPA20 exhibits a higher storage modulus (G′) than loss modulus (G″), indicating solid-like characteristics dominated by strong interparticle forces and elastic behavior. On the other hand, NPA50 and NPA72 show a higher G″ than G′, indicating liquid-like characteristics dominated by weak interparticle forces and viscous behavior. In particular, NPA72 exhibits a significant difference between G″ and G′, indicating relatively stronger liquid-like behavior. The results of viscoelastic behavior demonstrate that ink's structural characteristics vary significantly depending on the solvent composition. In the frequency sweep results in Fig. 3(e), NPA20 exhibits dominance in elastic behavior, NPA50 transitions from elastic to viscous behavior with increasing frequency, and NPA72 shows dominance in viscous behavior.

3. Crack Formation after Coating

The structure and rheological behavior of ink influence the formation of the microstructure of the catalyst layer during coating and drying processes, ultimately determining the performance and durability of the MEA. Therefore, understanding the correlation between the ink structure and the catalyst layer structure is another important research topic. Figs. 4(a)-(c) show the surface characteristics of electrode samples formed by directly coating ink on the electrolyte membrane to form the catalyst layer. As shown in Fig. 4(a), the coating state of the visible catalyst layer appears to be uniform, and the platinum loading measured by XRF shown in Fig. 4(b) also exhibits a uniform distribution. However, NPA20 appears to be brighter black compared to the other samples, indicating rel-

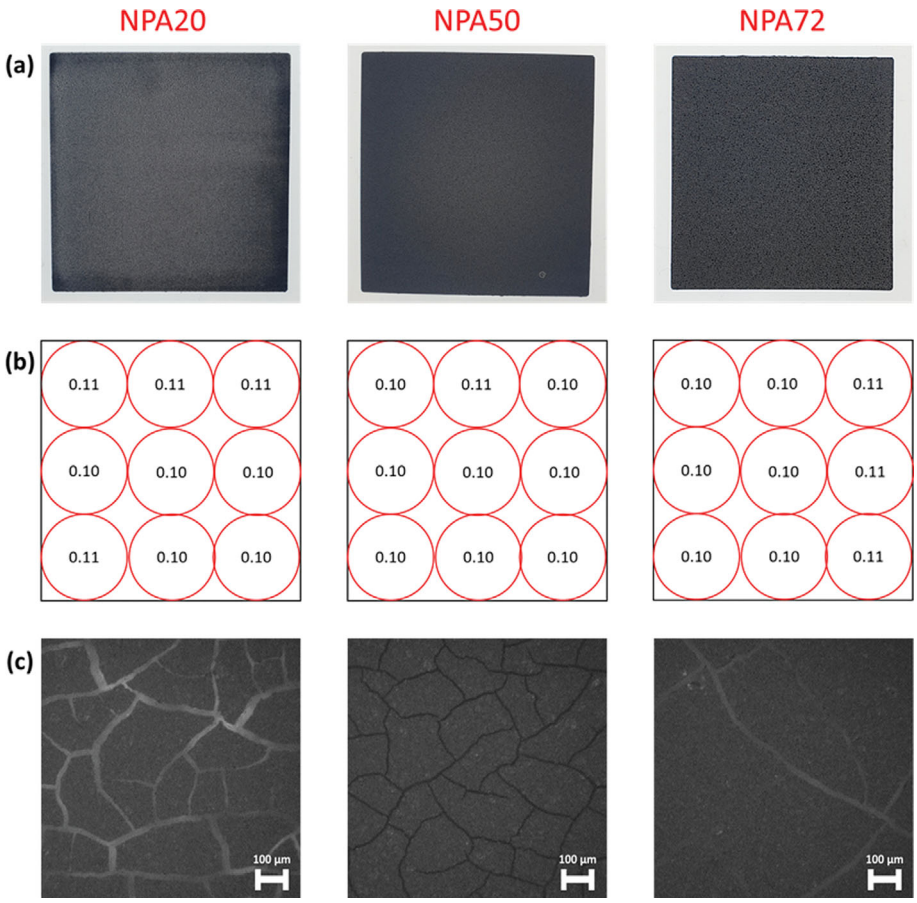

Fig. 4. (a) Images of catalyst layers formed on Nafion membrane. (b) The amount of Pt measured at nine different points on the surface of the MEAs. (c) Magnified image of the catalyst layer.

atively higher light transmittance in the NPA20 catalyst layer. As shown in the magnified image of the optical microscope in Fig. 4(c), the NPA20 catalyst layer exhibits the widest crack area due to a high frequency and large crack width, thereby affecting the brightness of the electrode surface. Conversely, NPA72 exhibits significantly less frequent crack formation. These results confirm that ink properties directly affect the crack formation behavior of the catalyst layer. The crack formation behavior dependent on ink structure will be discussed in more detail in the following section.

4. Influence of Solvent Composition on Ink Structure and Crack Formation in Catalyst Layer

In order to propose the solvent-dependence of ink structure and crack formation in the catalyst layer, results on sedimentation behavior, rheological properties, and crack characteristics of three different inks with varying solvent composition are presented in Fig. 5. It is speculated that in NPA20, which contains a large amount of water, ionomers adsorbed on the surface of catalyst particles form a three-dimensional network structure by utilizing the bridging effect of the adsorbed ionomers. Ink properties dominated by elasticity, as observed in the gel-like behavior, support this hypothesis. However, as seen in the shear thinning phenomenon, this network structure is weakly formed and can result in non-uniform agglomerate size due to partial dissolution by centrifugal or shear forces induced during sedimentation experiment or coating process. As a result, relatively non-uniform sedimentation and large crack formation in the catalyst layer are expected. During the solvent evaporation after ink coating, the non-uniformity in the agglomeration size of the catalyst layer can lead to non-uniformity in the pore structure and subsequently, to uneven drying stress. To relieve this stress, cracks are formed as a means of stress relief [9]. Additionally, the high viscosity of NPA20 can further contribute to non-uniformity in coating thickness and delay leveling. In contrast, in NPA72, which contains a relatively large amount of NPA compared to water, it is assumed that high affinity between solvent, catalyst, and ionomer leads to their dispersion in a well-dispersed state. Moreover, in NPA72, free ionomers mainly exist, interfering with the agglomeration of catalyst particles and forming a uniform ink structure. The rheological experiment supports this with low viscosity and liquid-like behavior. Therefore, the small and uniform catalyst particles and free ionomer composition in NPA72 reduce crack formation by balancing stress during drying, resulting in a uniform catalyst layer. Furthermore, the low viscosity of NPA72 facilitates smooth leveling after coating and improves uniformity in the catalyst layer. The crack characteristics of the catalyst layer formed differently depending on the solvent composition of the ink can directly affect the performance and durability of the fuel cell by damaging the catalyst layer/membrane interface and interfering with oxygen diffusion caused by changes in water manage-

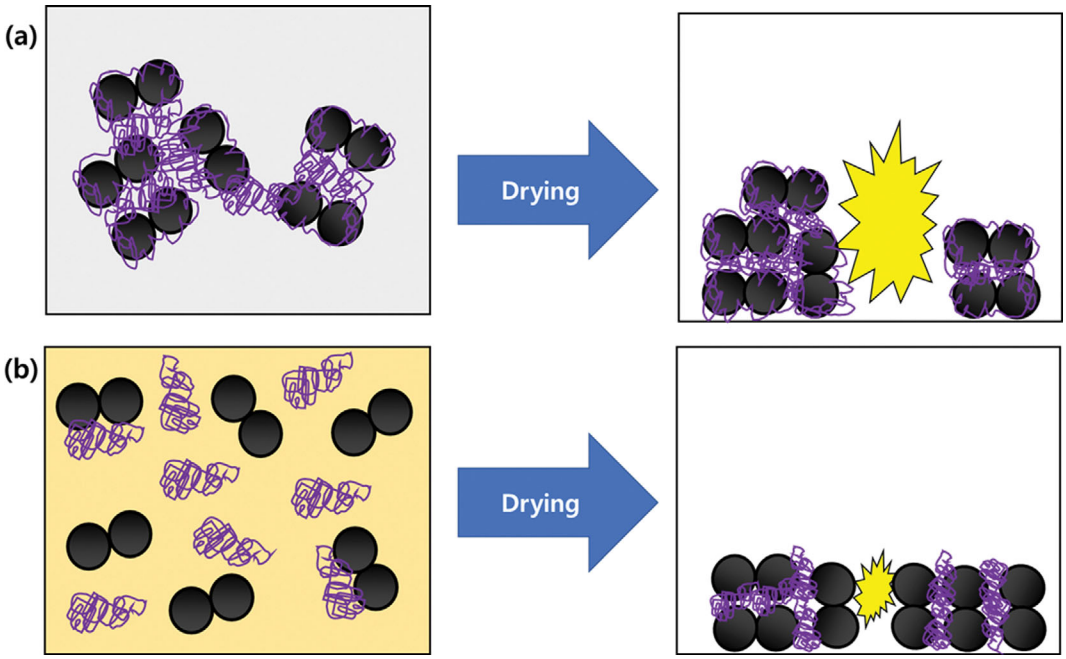

Fig. 5. Conceptual sketch of the ink structure and crack formation mechanism in the catalyst layer as a function of solvent properties. (a) NPA20. (b) NPA72, Black represents the catalyst, purple represents the ionomer, and yellow represents the crack.

ment in the catalyst layer [30,31]. Therefore, based on the present findings, a detailed study on the correlation between ink structure, catalyst layer cracks, and fuel cell performance will be conducted in the future.

CONCLUSIONS

Despite the use of the same catalyst and ionomer, the solvent composition significantly affects the structure of the ink and crack characteristics of the catalyst layer. Ink structure differences due to solvent composition could not be clearly observed by ink sedimentation behavior. On the other hand, rheological evaluations provided more specific information. NPA20, which has a high water content, exhibited shear thinning behavior and dominant elastic gel behavior. This suggests that NPA20 has a network structure formed by ionomers adsorbed on the catalyst surface. In contrast, NPA72, which has a high content of NPA, exhibited behavior close to that of a low viscosity Newtonian fluid or liquid. Thus, it was inferred that NPA72 has a structure in which the catalyst and ionomer are well dispersed in small sizes. Due to these ink structural differences, collapse of the NPA20 network structure and resulting uneven catalyst agglomeration during the coating process led to significant crack formation in the resulting catalyst layer. In contrast, crack formation significantly decreased in NPA72, which has a relatively uniform ink structure.

ACKNOWLEDGEMENTS

This work was supported by the Technology Innovation Program (20011712) funded by the Ministry of Trade, Industry and Energy (MOTIE, Korea). This work was also supported by the National Research Foundation of Korea (NRF) funded by the Ministry of Science, ICT & Future Planning (NRF-2020M1A2A2080796).

REFERENCES

1. M. Harada, S. Takata, H. Iwase, S. Kajiya, H. Kadoura and T. Kanaya, *ACS Omega*, **6**, 15257 (2021).
2. M. Shibayama, T. Matsunaga, T. Kusano, K. Amemiya, N. Kobayashi and T. Yoshida, *J. Appl. Polym. Sci.*, **131**, 39842 (2014).
3. R. Balu, N. R. Chondhury, J. P. Mata, L. de Campo, C. Rehm, A. J. Hill and N. K. Dutta, *ACS Appl. Mater. Interfaces*, **11**, 9934 (2019).
4. F. Xu, H. Y. Zhang, J. Ilavsky, L. Stanciu, D. Ho, M. J. Justice, H. I. Petrache and J. Xie, *Langmuir*, **26**, 19199 (2010).
5. F. Yang, L. Xin, A. Uzunoglu, Y. Qui, L. Staniu, J. Ilavsky, W. Li and J. Xie, *ACS Appl. Mater. Interfaces*, **9**, 6530 (2017).
6. S. Khandavalli, R. Iyer, J. H. Park, D. J. Myers, K. C. Neyerlin, M. Ulsh and S. A. Mauger, *Langmuir*, **36**, 12247 (2020).
7. M. Wang, J. H. Park, S. Kabir, K. C. Neyerlin, N. N. Kariuki, H. Lv, V. R. Stamenkovic, D. J. Myers, M. Ulh and S. A. Mauger, *ACS Appl. Energy Mater.*, **2**, 6417 (2019).
8. S. Takahashi, T. Mashio, N. Horibe, K. Akizuki and A. Ohma, *ChemElectroChem*, **2**, 1560 (2015).
9. N. Kumano, K. Kudo, A. Suda, Y. Akimoto, M. Ishii and H. Nakamura, *J. Power Sources*, **419**, 219 (2019).
10. S. Shukla, S. Bhattacharjee, A. Z. Weber and M. Secanell, *J. Electrochem. Soc.*, **164**, F600 (2017).
11. M. B. Dixit, B. A. Harkey, F. Shen and K. B. Hatzell, *J. Electrochem. Soc.*, **165**, F264 (2018).
12. S. Takahashi, J. Shimanuki, T. Mashio, A. Ohma, H. Tohma, A. Ishihara, Y. Ito, Y. Nishino and A. Miyazawa, *Electrochim. Acta*, **224**, 178 (2017).

13. S. A. Berlinger, B. D. McCloskey and A. Z. Weber, *ACS Energy Lett.*, **6**, 2275 (2021).
14. T. Mabuchi, S. F. Huang and T. Tokumasu, *Macromolecules*, **53**, 3273 (2020).
15. M. Ghelichi, K. Malek and M. H. Eikerling, *Macromolecules*, **49**, 1479 (2016).
16. A. Tarokh, K. Karan and S. Ponnurangam, *Macromolecules*, **53**, 288 (2020).
17. J. H. Lee, G. Doo, S. H. Kwon, S. Choi and H. T. Kim, *Sci. Rep.*, **8**, 10739 (2018).
18. S. Khandavalli, J. H. Park, N. N. Kariuki, D. J. Myers, J. J. Stickel, K. Hurst, K. C. Neyerlin, M. Ulsh and S. A. Mauger, *ACS Appl. Mater. Interfaces*, **10**, 43610 (2018).
19. E. Hoffmann, S. Zhang, M. Thoma, C. Damm and W. Peukert, *Particuology*, **44**, 7 (2019).
20. S. Bapat and D. Segets, *ACS Appl. Nano Mater.*, **3**, 7384 (2020).
21. A. Z. Tanning, S. Lee, S. Woo, S. H. Park, B. Bae and S. D. Yim, *J. Electrochem. Soc.*, **168**, 104506 (2021).
22. B. V. Derjaguin and L. Landau, *Prog. Surf. Sci.*, **43**, 30 (1993).
23. E. J. W. Verwey and J. T. G. Overbeek, *Theory of the stability of lyophobic colloids*, The Interaction of Sol Particles Having an Electric Double Layer, Elsevier, New York, NY, 20 (1948).
24. V. Runkana, P. Somasundaran and P. C. Kapur, *Chem. Eng. Sci.*, **61**, 182 (2006).
25. M. So, T. Ohnishi, K. Park, M. Ono, Y. Tsuge and G. Inoue, *Int. J. Hydrogen Energy*, **44**, 28984 (2019).
26. N. Kumano, K. Kudo, Y. Akimoto, M. Ishii and H. Nakamura, *Carbon*, **169**, 429 (2020).
27. A. K. Dolan and S. F. Edwards, *Proc. R. Soc. London*, **A337**, 509 (1974).
28. A. N. Semenov and A. A. Shvets, *Soft Matter*, **11**, 8863 (2015).
29. J. H. Lee, U. Paik, J. Y. Choi, K. K. Kim, S. M. Yoon, J. Lee, B. K. Kim, J. M. Kim, M. H. Park, C. W. Yang, K. H. An and Y. H. Lee, *J. Phys. Chem. C*, **111**, 2477 (2007).
30. Y. Qin, S. Ma, Y. Chang, Y. Liu, Y. Yin, J. Zhang, Z. Liu, K. Jiao and Q. Du, *Int. J. Hydrogen Energy*, **46**, 8722 (2021).
31. Y. Matsui, T. Suzuki, P. Deevanhxay, S. Tsushima and S. Hirai, ASME 2013 11th Int Conf Fuel Cell Sci Eng Technol. ASME, 1-5 (2013).